

# Accurate Measurement of Dynamic ON-state Resistances of GaN Devices under Reverse and Forward Conduction in High Frequency Power Converter

Ke LI, *IEEE Member*, Arnaud VIDET, *IEEE Member*, Nadir IDIR, *IEEE Member*, Paul EVANS, Mark JOHNSON, *IEEE Member*

**Abstract**—Because of trapped charges in GaN transistor structure, device dynamic ON-state resistance  $R_{\text{DSon}}$  is increased when it is operated in high frequency switched power converters, in which device is possibly operated by zero voltage switching (ZVS) to reduce its turn-ON switching losses. When GaN transistor finishes ZVS during one switching period, device has been operated under both reverse and forward conduction. Therefore its dynamic  $R_{\text{DSon}}$  under both conduction modes needs to be carefully measured to understand device power losses. For this reason, a measurement circuit with simple structure and fast dynamic response is proposed to characterise device reverse and forward  $R_{\text{DSon}}$ . In order to improve measurement sensitivity when device switches at high frequency, a trapezoidal current mode is proposed to measure device  $R_{\text{DSon}}$  under almost constant current, which resolves measurement sensitivity issues caused by unavoidable measurement circuit parasitic inductance and measurement probes deskew in conventional device characterisation method by triangle current mode. Proposed measurement circuit and measurement method is then validated by first characterising a SiC-MOSFET with constant  $R_{\text{DSon}}$ . Then, the comparison on GaN-HEMT dynamic  $R_{\text{DSon}}$  measurement results demonstrates the improved accuracy of proposed trapezoidal current mode over conventional triangle current mode when device switches at 1MHz.

**Index Terms**—GaN transistor, dynamic ON-state resistance, high switching frequency, reverse conduction, forward conduction, soft switching

## I. INTRODUCTION

Because of low power losses and fast switching transition, integrating gallium nitride (GaN) power semiconductor devices into high frequency electrical energy conversion systems is becoming a hot research topic [1]–[4] to increase power converter power density. To design high frequency power converters, device power losses estimation becomes very important, as it determines whole system cooling equipment size, which is a key factor to influence on system power density. However, unlike silicon (Si) or silicon carbide (SiC) devices, GaN device has an unwanted characteristic, which is caused by the trapped charge in device buffer layer when device is in OFF-state. Those trapped charges will reduce device current conduction capability, resulting in increased ON-state resistance ( $R_{\text{DSon}}$ ) compared with device theoretical value. It is to be noted that GaN device dynamic  $R_{\text{DSon}}$  values are normally not given in device datasheet, which makes its conduction power losses unpredictable in application. Further-

more, power semiconductor devices  $R_{\text{DSon}}$  is an important parameter for power electronics systems diagnosis, which can be used as an indicator to study the degradation of both device [5] and packaging [6]. Therefore, a clear understanding of GaN device dynamic  $R_{\text{DSon}}$  is also important for the study of power electronics systems health management. For those reasons, it is necessary to propose new characterisation method to accurately measure GaN device dynamic  $R_{\text{DSon}}$  in high frequency power converters.

Even though GaN device fabrication process has been improved by different techniques such as field-plate structure [7] and ameliorated device buffer layer [8], [9] to decrease dynamic  $R_{\text{DSon}}$  value, it is still found in reported research work [10]–[17] that commercial device dynamic  $R_{\text{DSon}}$  can increase to maximal 5-10 times bigger than device static  $R_{\text{DSon}}$  value depending on device operation conditions.

GaN device dynamic  $R_{\text{DSon}}$  measurement method reported in the above research work can be summarised into TABLE I, where there are in general indirect and direct measurement method. In indirect measurement method [10], whole system power losses is measured at first, then with knowledge of other losses present in the active and passive components, the device conduction losses can be indirectly obtained. However, the application of this method in device hard switching operation has not been discussed, as device hard switching losses might cause measurement sensitivity issue, which needs to be further investigated.

In direct measurement method, GaN device conduction current and voltage are measured to obtain  $R_{\text{DSon}}$ . As illustrated in Fig. 1a, measurement circuit is normally constituted by Device Switching Circuit (DSC), Device Under Test (DUT) and Voltage Clamping Circuit (VCC). The main purpose of DSC (including current source  $I_c$ ) is to control DUT OFF-state, ON-state time and switching conditions. The aim of VCC is to alter the voltage across DUT  $V_{\text{DS}}$  to the measured voltage  $V_{\text{DS(m.)}}$  by  $V_{\text{DS(m.)}} = V_{\text{DS}} - \Delta V$ , where  $\Delta V$  is the voltage across VCC.  $\Delta V$  should equal to  $V_{\text{DS}}$  when DUT is in OFF-state, while  $\Delta V$  should be almost zero when DUT is in ON-state for measurement accuracy. Therefore, instead of measuring full range  $V_{\text{DS}}$  voltage, smaller  $V_{\text{DS(m.)}}$  voltage is measured to improve the measurement resolution of the oscilloscope (with 8-bit to 12-bit resolution). It can be also noted that parasitic inductance  $L_c$  from DUT branch is

TABLE I: Comparison between the state-of-the-art research work and proposed method in this work to measure GaN device dynamic  $R_{DSon}$

| Research work  | Method   | Switching mode        | Current mode & device conduction    | Not discussed                   |
|--|----------|-----------------------|-------------------------------------|---------------------------------|
| Galapon et al. [10]  | Indirect | Soft switching        | Quasi sinusoidal, forward & reverse | Sensitivity, hard switching     |
| Badawi et al. [11], Cai et al., [12]<br>Yang et al. [13], Foulkes et al., [14]<br>Li et al. [15] | Direct   | Hard switching        | Quasi constant, forward             | Soft switching, reverse current |
| Lu et al. [16], Li et al. [17]   | Direct   | Hard & Soft switching | Triangular, forward                 | Sensitivity, reverse current    |
| <b>This work</b>   | Direct   | Hard & Soft switching | Trapezoidal, forward & reverse      | -                               |

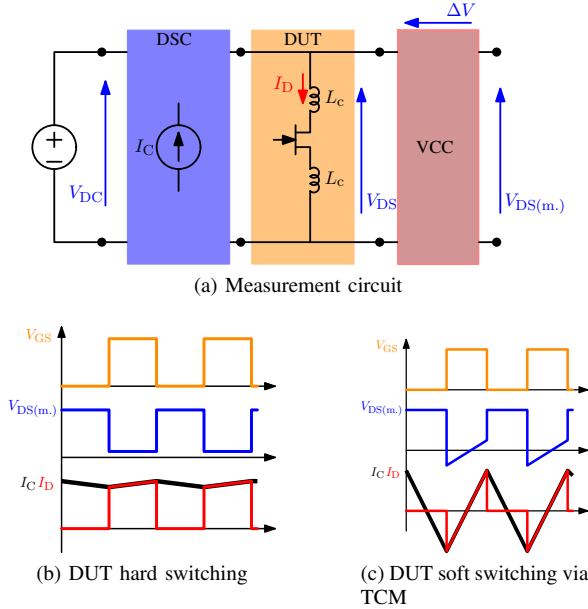


Fig. 1: Measurement circuit to measure GaN device dynamic  $R_{DSon}$  value

appeared in both DSC and VCC part, which is their common  $L_c$  when DUT is in operation.

In the published work [11]–[15], authors use different types of the circuit to investigate GaN device dynamic  $R_{DSon}$  value under hard switching condition, in which DUT gate source voltage  $V_{GS}$ ,  $V_{DS(m)}$  and drain current  $I_D$  waveform are shown in Fig. 1b (supposing  $I_C$  is in continuous mode). When DUT is in ON-state, it is always under forward conduction by a quasi constant  $I_D$ , therefore  $L_c$  has little influence on dynamic  $R_{DSon}$  measurement results. However, because device can only operate at hard switching in the presented measurement circuits, the above research work cannot be directly applied to investigate GaN device dynamic  $R_{DSon}$  value in soft switching condition, where DUT is under reverse conduction.

To extend the method to the case when GaN device is operated in soft switching condition, authors in [16], [17] have proposed a resonant tank in DSC and have controlled DUT in zero voltage switching (ZVS) via triangle current mode (TCM), in which its  $V_{GS}$ ,  $V_{DS(m)}$  and  $I_D$  waveform are shown in Fig. 1c. However, GaN device dynamic  $R_{DSon}$  is only measured under forward conduction in the above work. Additionally, measurement sensitivity issue due to voltage

drop  $V_{L_c}$  by  $I_D$  fast transition  $di/dt$  has not been discussed.

It is important to measure GaN device dynamic  $R_{DSon}$  when device is under reverse conduction for the following reasons.

- 1) Soft switching is an effective method to reduce GaN device switching losses, so device can operate in high frequency (HF) to improve power converter power density. It is necessary to know the dynamic  $R_{DSon}$  value immediately after device leaves the OFF-state and begins conduction, but in soft switching operation the device may be in a reverse conduction mode at this time. Only obtaining its dynamic  $R_{DSon}$  value under forward conduction may underestimate its conduction losses.
- 2) During deadtime between two transistors in a phase-leg, current flows reversely through one transistor after turn-OFF of the other. Therefore, it is important to understand this deadtime loss in HF power converters when using GaN devices [18], which requires VCC with reverse current blocking capability and low  $\Delta V$  under DUT reverse conduction.

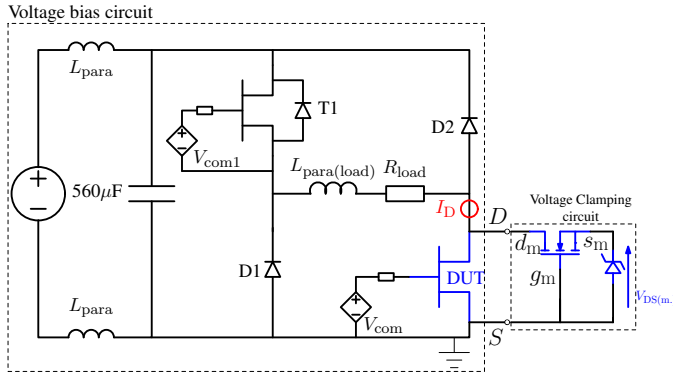
Therefore, the main objective of the paper is to accurately measure GaN device dynamic  $R_{DSon}$  under both reverse and forward conduction when device operates at HF converter. The main contributions are: 1) To propose a new VCC accordingly. 2) To study measurement accuracy and cause of the errors. 3) Measurement sensitivity issues are resolved by new trapezoidal current mode (TZCM), where device is still operated at soft switching in HF and it brings practical benefits by adding delay between two phase-legs.

As shown in TABLE II, the presented results in this paper extends device characterisation area in terms of switching frequency, measurement time and device operation conditions than our previous work presented in [15]. It is an overall achievement by using new measurement circuit and TZCM measurement method.

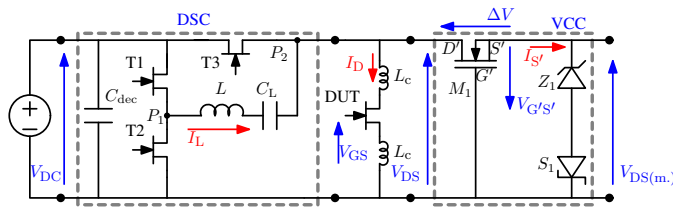
The paper is structured with following sections. In section II, new measurement circuit is proposed to characterise GaN device dynamic  $R_{DSon}$  value in both reverse and forward conduction. In section III, influence of measurement circuit  $L_c$  and other parameters (measurement probes skew and oscilloscope offset voltage) on GaN device dynamic  $R_{DSon}$  measurement sensitivity is studied and trapezoidal current mode is proposed. In section IV, experimental measurement results are presented to validate proposed measurement circuit and method. The paper is concluded in section V.

TABLE II: Comparison between our previous paper [15] and this paper

|                               | Previous paper                                  | This paper  |
|-------------------------------|---|---|
| Converter operation frequency | <10kHz, transient-state to 0.1s                 | until 1MHz, steady-state >100s                      |
| Purpose                       | Dynamic $R_{DSon}$ characterisation & modelling | Accurate dynamic $R_{DSon}$ characterisation        |
| Paper structure               | Characterisation circuit & modelling method     | Characterisation circuit & characterisation method  |
| Measurement time              | >1 $\mu$ s                                      | >10ns   |
| Operation conditions          | hard switching, forward conduction              | hard & soft switching, forward & reverse conduction |



(a) Measurement circuit of our previous work in [15] to measure GaN device dynamic  $R_{DSon}$  only under forward conduction



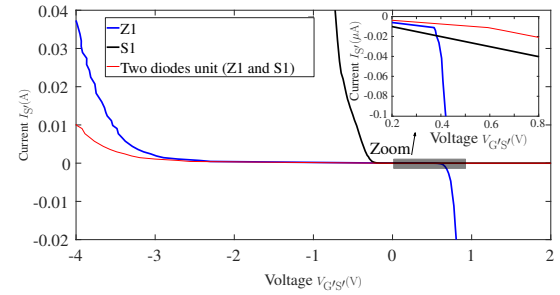
(b) Measurement circuit of this paper to measure GaN device dynamic  $R_{DSon}$  under reverse and forward conduction

Fig. 2: Comparison of the electrical circuit between our previous work and this work to measure GaN device dynamic  $R_{DSon}$

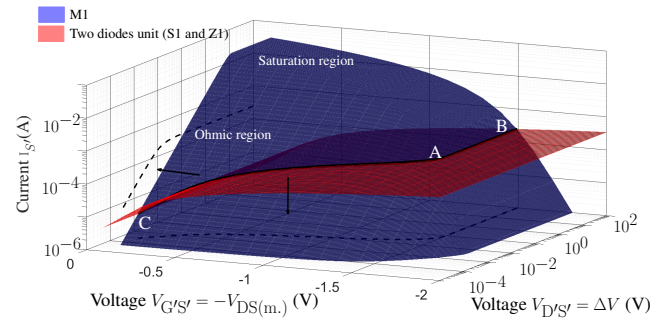
## II. MEASUREMENT CIRCUIT OF GAN DEVICE DYNAMIC $R_{DSon}$ UNDER REVERSE AND FORWARD CONDUCTION

### A. Measurement circuit

In our previously used electrical circuit shown in Fig. 2a [15], DUT can only operate in hard switching condition under forward conduction. In order to extend DUT operation conditions, another electrical circuit shown in Fig. 2b is proposed in this paper, where GaN device dynamic  $R_{DSon}$  value under both reverse and forward conduction can be characterised. In this circuit, the DSC part is a standard H-bridge circuit with two phases including decoupling capacitor  $C_{dec}$ , three identical power semiconductor devices T1, T2, T3. By connecting an output inductor  $L$  and capacitor  $C_L$  between nodes  $P_1$  and  $P_2$ , DUT can operate at soft switching by alternating inductor current  $I_L$  direction. VCC part is constituted by three main components: a depletion-mode MOSFET  $M_1$  with threshold voltage ( $V_{th}$ ) inferior to zero, a Zener diode  $Z_1$  and a Schottky diode  $S_1$ . The measured voltage  $V_{DS(m)}$  is between cathode (K) of  $Z_1$  and cathode of  $S_1$ , which also equals to the reverse gate voltage  $V_{G'S'}$  of  $M_1$  ( $V_{G'S'} = -V_{DS(m)}$ ). Following chosen components are chosen in the VCC part: M1 (BSP135,



(a) Two diodes unit characteristics



(b) M1 and two diodes unit characteristics

Fig. 3: VCC static characteristics

600V/100mA,  $V_{th} \approx -1.6V$ ), Z1 (BZT52C3V3, Zener voltage is 3.3V) and S1 (RB751SM-40FH, 40V/30mA). The choice of those components is justified by the circuit analysis below.

The relation of current and voltage of each diode Z1 and S1 together with their unit characteristics under their connection is shown in  $V_{G'S'}-I_{S'}$  plot in Fig. 3a. It is to be noted that for the chosen components, M1 gate leakage current can be neglected in comparison with two diodes unit leakage current. Two diodes unit static characteristic is then represented in the form of a surface in Fig. 3b.

Static characteristics of M1 is also represented in Fig. 3b in the form of a surface, where M1 ohmic region and saturation region are illustrated.  $\Delta V$  equals to  $V_{D'S'}$  voltage, which defines the measurement error when DUT is in ON-state.

It can be observed that there is an intersection line between two surfaces, which represents common static characteristics of M1 and two diodes unit. Depending on DUT operation conditions, static characteristics of VCC follows this intersection line.

- DUT OFF-state: Static characteristics of VCC is in intersection line AB. It is shown that  $V_{G'S'}$  voltage is around M1  $V_{th}$ , so M1 is in OFF-state and it withstands almost the whole DC voltage ( $\Delta V \approx V_{DC}$ ). Measured  $V_{DS(m)}$

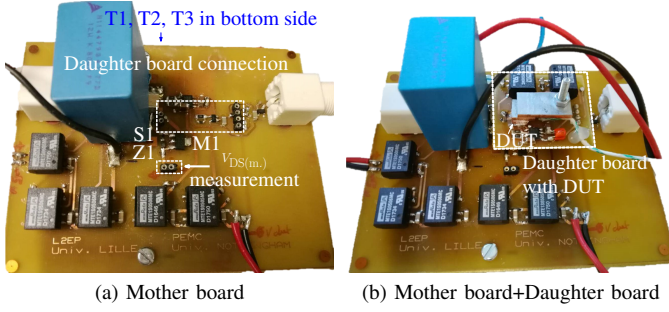


Fig. 4: Measurement circuit realization

is around M1 opposite  $V_{th}$  value. In this condition, as shown in the projection of line AB in  $I_{S'}-V_{D'S'}$  plane, leakage current of the chosen components in the VCC part is about  $200\mu A$ , which will not cause components self-heating.

- DUT forward conduction: Static characteristics of VCC part is in intersection line AC. As long as DUT forward ON-state voltage  $V_{DSon(F.)}$  is inferior to M1 opposite  $V_{th}$ , M1 operates in the ohmic region. As shown in the projection of line AC in  $V_{G'S'}-V_{D'S'}$  plane,  $\Delta V$  is much smaller than measured voltage  $V_{DS(m.)}$  ( $\Delta V = 10mV$  when  $V_{DS(m.)} = 1V$ ). Therefore,  $V_{DS(m.)}$  equals to DUT forward ON-state voltage  $V_{DSon(F.)}$ .
- DUT reverse conduction:  $V_{G'S'}$  voltage is positive in this condition, so M1 operates at ohmic region (ON-state resistance less than  $50\Omega$ ). As reverse  $I_{S'}$  is very small (less than  $0.1\mu A$ , see Fig. 3a),  $\Delta V$  is less than  $5\mu V$ . Therefore, similar as DUT forward conduction, measured voltage  $V_{DS(m.)}$  equals to DUT reverse ON-state voltage  $V_{DSon(R.)}$ .

Regarding the measurement accuracy, it can be noted that the proposed VCC is robust on drift of any temperature-dependent device static characteristics and it does not require any calibration of chosen devices, which is the case for using diode-type VCC in the literature [17]. Furthermore, it has reverse current blocking capability, which guarantees a wide operation range when DUT is under reverse conduction and during deadtime.

In terms of dynamic characteristics, proposed VCC improves the circuit dynamic response and M1 gate voltage overshoot, which is major drawback of transistor-type VCC analyzed by Gelagaev et al. in [19].

- DUT OFF-ON transition: As  $V_{G'S'}$  is around M1  $V_{th}$  value when DUT is in OFF-state, M1 gate source capacitance  $C_{G'S'}$  only needs a little charge (less than  $0.1nC$ ) to increase  $V_{G'S'}$  voltage superior to  $V_{th}$  during DUT ZVS transition. When  $V_{G'S'}$  is superior to  $V_{th}$ , M1 output capacitance stored charge  $Q_{oss'}$  (about  $2nC$  when DUT switches at 200V) is dissipated in M1 channel quickly. Therefore, dynamic response of the VCC is fast to follow DUT OFF-ON transition.  $Q_{oss'}$  of M1 is inferior to 20% of that of chosen DUT, which makes proposed VCC non-intrusive during measurement. Minimum  $V_{DS(m.)}$  is determined by whether DUT body diode conducts during

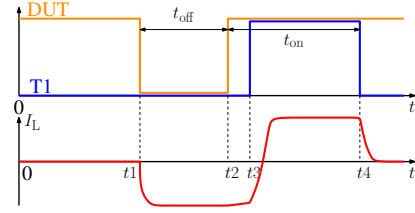


Fig. 5: Single-pulse control signal to measure power transistor reverse and forward ON-state resistance

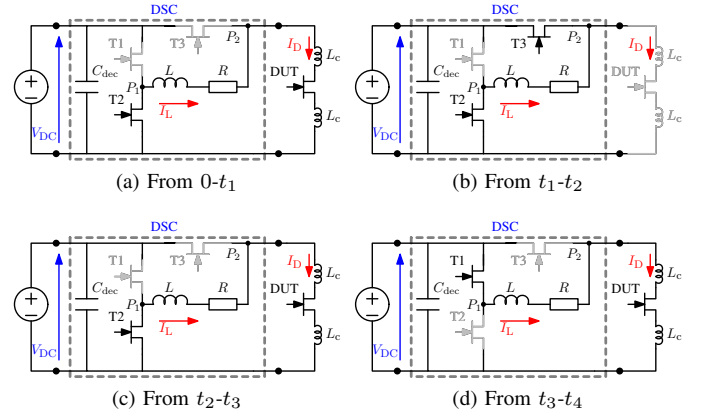


Fig. 6: Different circuit operation stages under given single-pulse control signal

deadtime, which is normally a voltage drop of 2-3 V.

- DUT ON-OFF transition: Maximum  $V_{DS(m.)}$  is determined by  $V_{G'S'}$  overshoot voltage during transition, where it is clamped by the chosen Z1 (3.3V). As S1 has very small ON-state voltage drop, total overshoot voltage is inferior to 4V during DUT transition, which improves M1 gate voltage surge immunity.

It can be concluded that in all the above DUT operation conditions, measured  $V_{DS(m.)}$  equals to the  $V_{G'S'}$  variation, which is from a few negative volts (bigger than -3V) to a few positive volts (less than 4V). Therefore, a small voltage division (500mV/div or 1V/div) of the oscilloscope can be used in the measurement to have an improved resolution on  $V_{DSon}$  value compared with a direct measurement (with 50V/div or 100V/div).

Measurement circuit is realized with the photo shown in Fig. 4, where it is constituted by a mother board including same GaN-HEMT T1, T2, T3 (GS66502B, 650V/7.5A) with their gate drivers, alongside M1, Z1, S1 of VCC part and a daughter board including DUT with its gate driver. The advantage of this design is that only daughter board needs to be changed to characterise different types of DUT.

Validation of the circuit when device is operated at hard switching has been presented in [15]. Therefore, in this paper, measurement results are focused on device soft switching operation.

### B. Measurement circuit validation

By replacing  $LC_L$  by a  $RL$  branch between  $P_1$  and  $P_2$  at first in Fig. 2b, a SiC-MOSFET (C2M0160120D, 1200V/19A,

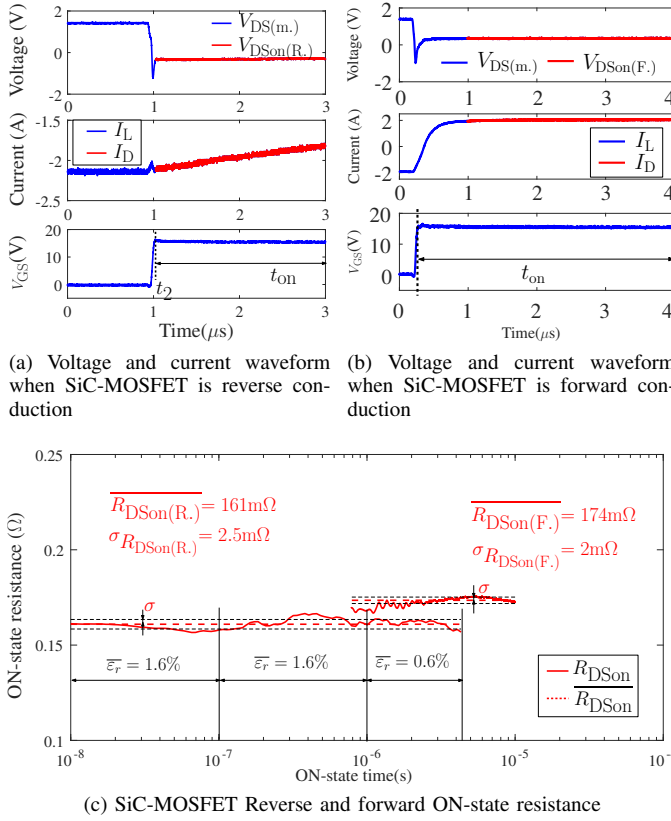


Fig. 7: SiC-MOSFET reverse and forward ON-state resistance measurement results

TABLE III: Comparison of SiC-MOSFET  $\overline{R_{DSon(R.)}}$  and  $\overline{R_{DSon(F.)}}$  between proposed method and device curve tracer

|                            | $\overline{R_{DSon(R.)}}$ | $\overline{R_{DSon(F.)}}$ |
|----------------------------|---------------------------|---------------------------|
| Proposed method            | 161 m $\Omega$            | 174m $\Omega$             |
| Device curve tracer        | 163 m $\Omega$            | 169 m $\Omega$            |
| Relative measurement error | 1.2%                      | 2.9%                      |

$V_{th} = 2.6\text{V}$ ) with static  $R_{DSon}$  around  $200\text{m}\Omega$  is characterised first by the above measurement circuit with single-pulse control signals of T1 and DUT given in Fig. 5. T2 and T3 are complimentary control signals of T1 and DUT respectively.

From  $0-t_1$  (see Fig. 6a), both DUT and T2 are in ON-state, therefore  $I_L = 0$ . Afterwards, both T3 and T2 are in ON-state from  $t_1-t_2$  (see Fig. 6b), where  $I_L$  is charged in reverse conduction until steady state. DUT OFF-state time  $t_{off}$  is defined by this interval. Following that, both DUT and T2 are in ON-state from  $t_2-t_3$  (see Fig. 6c), where DUT is turned on at ZVS at  $t_2$  and it begins conducting reversely  $I_L$  ( $I_L$  decreases towards zero with time constant  $\frac{L}{R}$ ). At final step  $t_3-t_4$  (see Fig. 6d), both DUT and T1 are in ON-state, where  $I_L$  alternates direction until steady state in forward conduction (time constant is still determined by  $\frac{L}{R}$ ). Thus, DUT ON-state time  $t_{on}$  is defined by  $t_2-t_4$  interval. A detailed analysis on DUT ZVS process has been presented by authors in [20]. Under this control sequence, DUT  $R_{DSon}$  under reverse and forward conduction ( $R_{DSon(R.)}$  and  $R_{DSon(F.)}$ )

can be obtained at  $t_2-t_3$  interval and  $t_3-t_4$  interval respectively under constant  $I_L$ .  $R_{DSon(R.)}$  can be obtained under long  $t_{on}$  by choosing a big  $L$  and  $R_{DSon(F.)}$  can be obtained quickly after  $I_L$  transition by using a small  $L$ . Therefore, by setting  $t_2-t_3$  stage length accordingly, both  $R_{DSon(R.)}$  and  $R_{DSon(F.)}$  can be obtained under similar  $t_{on}$  scale to compare.

As SiC-MOSFET does not suffer any dynamic resistance variation as GaN transistor, its obtained reverse and forward ON-state resistance by the proposed circuit can be used as a reference to verify proposed circuit dynamic response and accuracy. Measurement condition is:  $V_{DC} = 200\text{V}$  and stabilized DUT ON-state current is 2A.  $I_L$  is obtained in experiment measurement, and  $I_L = I_D$  when DUT  $V_{GS}$  reaches ON-state gate voltage.

For the characterised SiC-MOSFET, as shown in Fig. 7a when DUT is in OFF-state, obtained  $V_{DS(m.)}$  is clamped to reverse  $V_{th}$  of chosen depletion MOSFET ( $V_{th} \approx -1.6\text{V}$ ), which confirms the above circuit analysis and when it is under reverse conduction, DUT reverse ON-state voltage  $V_{DSon(R.)}$  and current  $I_D$  can be measured quickly after  $V_{GS} = 16\text{V}$ , which confirms the fast response of the presented measurement circuit. As shown in Fig. 7b when it is under forward conduction, DUT forward ON-state voltage  $V_{DSon(F.)}$  and current  $I_D$  are measured when  $I_L$  is stabilized.

DUT  $R_{DSon(R.)}$  and  $R_{DSon(F.)}$  are then compared in Fig. 7c to show its variation with ON-state time  $t_{on}$ . Obtained DUT average reverse ON-state resistance ( $\overline{R_{DSon(R.)}}$ ) by the proposed measurement method is about  $161\text{m}\Omega$ , even with some noise on the measurement data,  $R_{DSon(R.)}$  standard derivation ( $\sigma_{R_{DSon(R.)}}$ ) is about  $2.5\text{m}\Omega$ , which is only 1.6% to  $\overline{R_{DSon(R.)}}$ . In terms of DUT average forward ON-state resistance ( $\overline{R_{DSon(F.)}}$ ), obtained value is about  $174\text{m}\Omega$  with  $2\text{m}\Omega$  on  $\sigma_{R_{DSon(F.)}}$  (1.1% to  $\overline{R_{DSon(F.)}}$ ). Those small relative  $\sigma_{R_{DSon(R.)}}$  and  $\sigma_{R_{DSon(F.)}}$  values prove the measurement consistency of the proposed circuit.

$\overline{R_{DSon(R.)}}$  and  $\overline{R_{DSon(F.)}}$  between proposed method is then compared in TABLE III with their values obtained in device curve tracer (B1505A). Relative measurement error between the proposed method to the curve tracer is inferior to 2.9%, which confirms the measurement accuracy of the proposed circuit. It is to be noted that for SiC-MOSFET, obtained device  $\overline{R_{DSon(R.)}}$  is slightly smaller than  $\overline{R_{DSon(F.)}}$ . This difference is supposed to be the SiC-MOSFET body diode conduction when DUT is under reverse conduction, which lowers DUT reverse  $R_{DSon(R.)}$ .

Response time of VCC is an important parameter to judge if it can be used to measure DUT dynamic  $R_{DSon}$  when DUT is applied in high frequency converter, no matter it is under soft or hard switching. To verify fast response of proposed VCC, the term of relative measurement error ( $\varepsilon_r = \frac{|R_{DSon(R.)}(t) - \overline{R_{DSon(R.)}}|}{\overline{R_{DSon(R.)}}}$ ) is used. Its average value ( $\overline{\varepsilon_r}$ ) of different time intervals ( $10\text{ns} \sim 100\text{ns}$ ,  $100\text{ns} \sim 1\mu\text{s}$  and after  $1\mu\text{s}$ ) are then compared in Fig. 7c.  $\overline{\varepsilon_r}$  is inferior to 1.6% when  $t_{on}$  is longer than  $10\text{ns}$ , which confirms fast dynamic response of proposed VCC to obtain DUT  $R_{DSon}$  when DUT switches in megahertz range power converter.

The proposed circuit is validated in this section and a control

signal of trapezoidal current mode will be presented in the next section to improve measurement sensitivity when device switches in high frequency converter.

### III. MEASURING GAN DEVICE DYNAMIC $R_{\text{DSon}}$ IN HIGH FREQUENCY CONVERTER

The conventional device characterisation method based on triangle current mode (TCM) is used to measure GaN device dynamic  $R_{\text{DSon}}$  when device operates in high frequency converter [17], [21]. Measurement error caused by unavoidable circuit parasitic inductance  $L_c$  under TCM on device ON-state resistance has been raised by authors in [21]. However, there is no solution proposed to compensate the measurement error. In this section, different sensitivity issues caused by unavoidable  $L_c$  and measurement probes deskew are studied. In order to improve measurement sensitivity when device is operated in high frequency power converter, a trapezoidal current mode (TZCM) is proposed accordingly.

#### A. Triangle current mode

Under  $I_D$  current fast transition of TCM, the influence of unavoidable  $L_c$  (see Fig. 2b) due to PCB tracks, device packaging etc., deskew ( $t_{\text{dk}}$ ) between voltage probe and current probe, and oscilloscope offset voltage accuracy ( $V_{\text{off}}$ , due to internal offset voltage source precision [22]) on dynamic  $R_{\text{DSon}}$  measurement sensitivity needs to be carefully studied when DUT is operated in high frequency converter.

Real DUT  $R_{\text{DSon}}$  is defined by:

$$R_{\text{DSon}}(t) = \frac{V_{\text{DSon}}(t)}{I_D(t)} \quad (1)$$

By considering the presence of  $L_c$  and oscilloscope offset  $V_{\text{off}}$ , measured apparent voltage  $V_{\text{DSon(m.)}}$  is:

$$V_{\text{DSon(m.)}}(t) = I_D(t) \cdot R_{\text{DSon}}(t) + L_c \frac{dI_D(t)}{dt} + V_{\text{off}} \quad (2)$$

By considering  $t_{\text{dk}}$  between current probe and voltage probe, relation between measured apparent current  $I_{\text{D(m.)}}(t)$  and real current  $I_D(t)$  can then be further expressed by:

$$I_{\text{D(m.)}}(t) = I_D(t) - t_{\text{dk}} \cdot \frac{dI_D(t)}{dt} \quad (3)$$

By combining eq.(2) and eq.(3) together, relative measurement error is therefore obtained by:

$$\begin{aligned} \varepsilon_r = & \frac{R_{\text{DSon(m.)}}(t) - R_{\text{DSon}}(t)}{R_{\text{DSon}}(t)} = f(L_c, t_{\text{dk}}, V_{\text{off}}) = \\ & \frac{t_{\text{dk}}}{I_{\text{D(m.)}}(t)} \cdot \frac{dI_D(t)}{dt} + \frac{L_c}{R_{\text{DSon}}(t) \cdot I_{\text{D(m.)}}(t)} \cdot \frac{dI_D(t)}{dt} \\ & + \frac{V_{\text{off}}}{R_{\text{DSon}}(t) \cdot I_{\text{D(m.)}}(t)} \end{aligned} \quad (4)$$

Supposing a symmetrical TCM is applied with  $D=50\%$  and  $I_{\text{D(m.)}}(t)$  is measured at its maximal value, following term  $\frac{1}{I_{\text{D(m.)}}(t)} \cdot \frac{dI_D(t)}{dt}$  can be simplified into  $4f_{\text{sw}}$ , which is only dependent on DUT switching frequency  $f_{\text{sw}}$ . The

influence of each variable  $L_c$ ,  $t_{\text{dk}}$  and  $V_{\text{off}}$  on  $\varepsilon_r$  is obtained by partial derivative of the function  $f(L_c, t_{\text{dk}}, V_{\text{off}})$ . They are then compared by following equations:

$$\begin{aligned} g_{t_{\text{dk}}} &= \frac{\partial f(t_{\text{dk}}, L_c, V_{\text{off}})}{\partial t_{\text{dk}}} = 4f_{\text{sw}} \\ g_{L_c} &= \frac{\partial f(t_{\text{dk}}, L_c, V_{\text{off}})}{\partial L_c} = \frac{4f_{\text{sw}}}{R_{\text{DSon}}(t)} \\ g_{V_{\text{off}}} &= \frac{\partial f(t_{\text{dk}}, L_c, V_{\text{off}})}{\partial V_{\text{off}}} = \frac{1}{R_{\text{DSon}}(t) \cdot I_{\text{D(m.)}}(t)} \end{aligned} \quad (5)$$

Supposing DUT switches at 1MHz, measured  $I_{\text{D(m.)}}(t)$  is about 2A and  $R_{\text{DSon}}(t)$  is about  $0.2\Omega$  (same condition as results presented in section II-B). The influence of each term on measurement error is obtained below.

- $g_{t_{\text{dk}}}$ : the influence of  $t_{\text{dk}}$  on measurement error shows directly proportional dependency on DUT switching frequency. When  $f_{\text{sw}} = 1\text{MHz}$ ,  $g_{t_{\text{dk}}} = 0.004/\text{ns}$ , which means  $1\text{ns}$  of uncorrected deskew between voltage and current probes results in 0.4% measurement error. Even though different probes deskew detecting methods have been analyzed in [23], it still needs special caution to accurately obtain this value.
- $g_{L_c}$ : the influence of  $L_c$  on measurement error shows directly proportional dependency on DUT switching frequency and inversely proportional dependency on DUT  $R_{\text{DSon}}$  value. For the characterised DUT as an example,  $g_{L_c} = 0.02/\text{nH}$ , which means  $1\text{nH}$  of unknown  $L_c$  value results in 2% measurement error. It is to be noted that part of  $L_c$  is from DUT packaging, which is not always an obvious parameter for power electronics engineers.
- $g_{V_{\text{off}}}$ : the influence of  $V_{\text{off}}$  on measurement error shows inversely proportional dependency on DUT  $R_{\text{DSon}}$  value and switching current. In the chosen example,  $g_{V_{\text{off}}} = 0.0025/\text{mV}$ , which means  $1\text{mV}$  of oscilloscope offset voltage error results in 0.25% measurement error. It is to be noted that unlike  $g_{t_{\text{dk}}}$  and  $g_{L_c}$ ,  $g_{V_{\text{off}}}$  is not dependent on  $f_{\text{sw}}$  and it is only determined by oscilloscope vertical voltage range setting, of which the value can be easily calibrated.

In the experimental work of this paper, measurement oscilloscope is 8-bit with 1GHz bandwidth (DPO4104B). A Hall effect current probe (100MHz, 1A/V) is used to measure  $I_L$  and a passive voltage probe (500MHz) is used to measure  $V_{\text{DS(m.)}}$ .  $t_{\text{dk}}$  of chosen probes is around  $10\text{ns}$ ,  $L_c$  is estimated to be  $10\text{nH}$  and  $V_{\text{off}}$  is within 1.5% of full voltage range (5V with 500mV/div). Therefore, each measurement error is:  $g_{t_{\text{dk}}} = 4\%$ ,  $g_{L_c} = 20\%$  and  $g_{V_{\text{off}}} = 19\%$ . It is to be noted that DUT can be placed at the same board with DSC and VCC to reduce  $L_c$ . However, it is not convenient in this design to characterise different devices.

Thus, total measurement error by applying the error propagation is:

$$g_{\text{total}} = \sqrt{g_{t_{\text{dk}}}^2 + g_{L_c}^2 + g_{V_{\text{off}}}^2} \approx 28\% \quad (6)$$

It is shown from the above analysis that special caution is necessary to measure DUT  $R_{\text{DSon}}$  under TCM, which requires

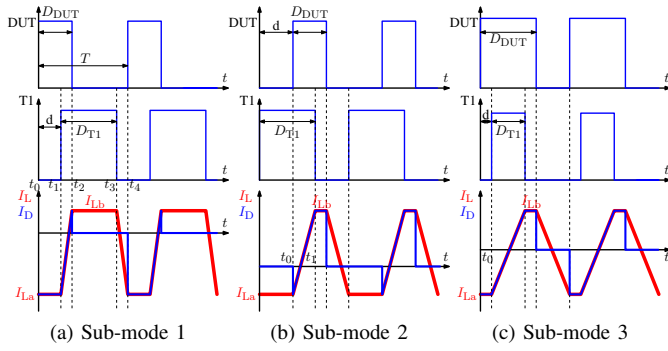


Fig. 8: Three current sub-modes of trapezoidal current mode

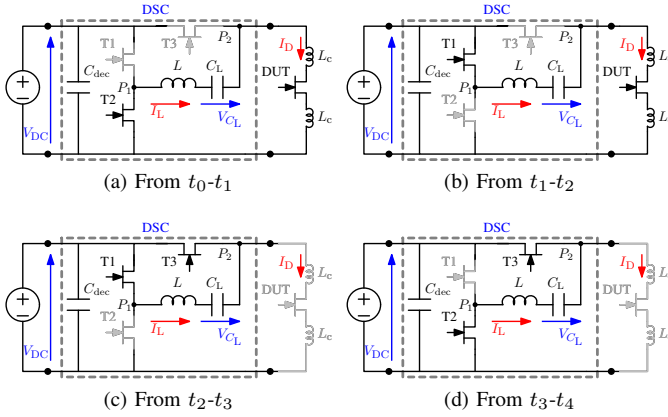


Fig. 9: Different circuit operation stages under sub-mode1 of TZCM

additional knowledge to accurately obtain  $t_{dk}$  and  $L_c$  and exclude their influence on obtained  $R_{DSon}$ . In order to improve measurement accuracy, it is proposed in the next subsection to measure DUT  $R_{DSon}$  under TZCM.

### B. Trapezoidal current mode

Unlike TCM, where DUT and T1 share the same control signal, control signal of T1 is different from DUT in TZCM. As DSC is a standard H-bridge, a phase shift  $d$  is applied between two legs. Ignoring effect of parasitic inductance  $L_c$ , when circuit is operated under TZCM, it should be ensured that there is no voltage across  $L$  when both legs are in the same switching state (“DUT ON, T1 OFF” and “DUT OFF, T1 ON”). Since these states correspond to nodes  $P_1$  and  $P_2$  having the same potential, this implies that there is no net voltage across capacitor  $C_L$  ( $V_{C_L} = 0$ ). Consequently, both legs must be controlled with the same duty cycle:  $D_{T1} = D_{T3}$ , which means  $D_{T1} + D_{DUT} = 1$ . When the two legs are in different switching states,  $V_{DC}$  is applied across  $L$  with phase shift controlling the amplitude of  $I_L$  trapezoidal waveform. Depending on DUT duty cycle ( $D_{DUT}$ ), there are three current sub modes in TZCM method, which is illustrated in Fig. 8. T2 and T3 are still complementary control signals of T1 and DUT respectively with a deadtime  $\tau$ . As  $\tau$  is much smaller than switching period, it is neglected in the analysis.

- 1) Sub-mode 1: From  $t_0-t_1$  (see Fig. 9a): DUT is turned on by negative load current  $I_{La}$  at  $t_0$  in ZVS. As T1 is delayed to DUT control signal by  $d$ , DUT is in reverse conduction by an almost constant  $I_{La}$  during the delay time. Therefore, DUT  $R_{DSon(R.)}$  can be measured under  $I_{La}$ . From  $t_1-t_2$  (see Fig. 9b): both DUT and T1 are in ON-state, therefore  $I_L$  is charged by  $V_{DC}$  at this stage. From  $t_2-t_3$  (see Fig. 9c): both T1 and T3 are in ON-state,  $I_L$  is with almost constant value  $I_{Lb}$ . From  $t_3-t_4$  (see Fig. 9d): both T2 and T3 are in ON-state,  $I_L$  is thus reversely charged by  $V_{DC}$ . Therefore, following two equations are applied:

$$V_{DC} = L \cdot \frac{(I_{Lb} - I_{La}) \cdot f_{sw}}{D_{DUT} - d} \quad (7)$$

$$I_{La} \cdot d + I_{Lb} \cdot (D_{T1} - (D_{DUT} - d)) + (I_{La} + I_{Lb}) \cdot (D_{DUT} - d) = 0$$

By simplifying eq.(7),  $I_{La}$  can be expressed by:

$$I_{La} = -\frac{V_{DC} \cdot (D_{DUT} - d)}{f_{sw} \cdot L} \cdot D_{T1} \quad (8)$$

- 2) Sub-mode 2: Control signal of DUT is delayed to T1 by  $d$ , so DUT is turned on by negative load current  $I_{La}$  at  $t_0$  in ZVS. As both T1 and DUT remain ON-state afterwards,  $I_L$  is charged by  $V_{DC}$  to alternate direction. When T1 is turned off at  $t_1$ , DUT is in forward conduction by an almost constant  $I_{Lb}$  until it is turned off. Therefore, DUT  $R_{DSon(F.)}$  can be measured under  $I_{Lb}$ . Following two equations are applied:

$$V_{DC} = L \cdot \frac{(I_{Lb} - I_{La}) \cdot f_{sw}}{D_{T1} - d} \quad (9)$$

$$I_{La} \cdot d + I_{Lb} \cdot (D_{DUT} - (D_{T1} - d)) + (I_{La} + I_{Lb}) \cdot (D_{T1} - d) = 0$$

$I_{Lb}$  can then be expressed by:

$$I_{Lb} = \frac{V_{DC} \cdot (D_{T1} - d)}{f_{sw} \cdot L} \cdot D_{T1} \quad (10)$$

- 3) Sub-mode 3: DUT is turned on by negative load current  $I_{La}$  at  $t_0$  in ZVS. Similar as sub-mode 1, DUT  $R_{DSon(R.)}$  can be measured under an almost constant  $I_{La}$  until T1 is turned on.  $I_L$  is charged by  $V_{DC}$  to alternate direction during T1 ON-state. Afterwards, similar as sub-mode 2, DUT  $R_{DSon(F.)}$  can be measured under an almost constant  $I_{Lb}$ . Following two equations are applied:

$$V_{DC} = L \cdot \frac{(I_{Lb} - I_{La}) \cdot f_{sw}}{D_{T1}} \quad (11)$$

$$I_{La} \cdot d + I_{Lb} \cdot (D_{DUT} - (D_{T1} + d)) + (I_{La} + I_{Lb}) \cdot D_{T1} = 0$$

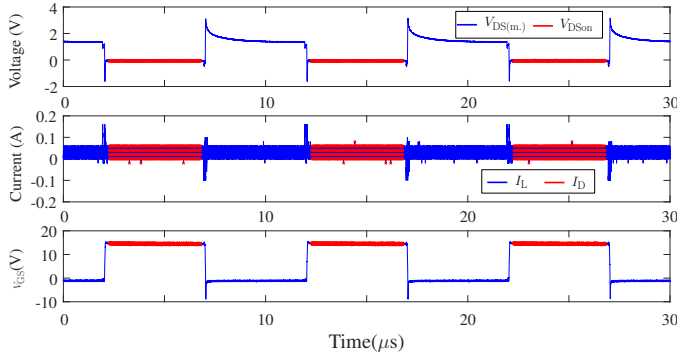


Fig. 10: Obtained device  $V_{DS(m.)}$ ,  $I_D$  and  $V_{GS}$  waveform to calibrate oscilloscope  $V_{off}$

$I_{La}$  and  $I_{Lb}$  can then be expressed by:

$$\begin{aligned} I_{La} &= -\frac{V_{DC} \cdot (D_{DUT} - d)}{f_{sw} \cdot L} \cdot D_{T1} \\ I_{Lb} &= \frac{V_{DC} \cdot (D_{T1} + d)}{f_{sw} \cdot L} \cdot D_{T1} \end{aligned} \quad (12)$$

By adding one degree of liberty  $d$  in TZCM,  $R_{DSon(R.)}$  and  $R_{DSon(F.)}$  can be measured under same  $I_{La}$  and  $I_{Lb}$  value with a constant  $L$  value in different  $f_{sw}$  and  $D_{DUT}$ , which is not the case by TCM method, where  $L$  value needs to be changed with  $f_{sw}$  and  $D_{DUT}$  to keep load current constant.

It is to be noted that for safety reason, it is preferred to add an external capacitor  $C_L$  in the circuit to withstand any unbalanced average voltage between  $P_1$  and  $P_2$  to be applied to  $L$ , which may result in infinite increase of  $I_L$ . Unbalanced average voltage may be caused by inhomogeneous delays in the gate driver of each transistor (it may slightly influence on  $D_{DUT}$  and  $D_{T1}$ ), ON-state voltage drops of the transistors and deadtime of two transistors of each bridge (it may slightly influence on each stage length). The resulting  $V_{C_L}$  value can be neglected in all the experimental results, so  $I_L$  is still under trapezoidal waveform, which can be proved by measurement results presented in section IV of the paper.

It can be also concluded that unlike TCM method, DUT  $R_{DSon}$  is measured at constant load current, which simultaneously resolves two of the measurement sensitivity issues highlighted in section III-A regarding the influence of measurement probe  $t_{dk}$  and of parasitic circuit and package inductance  $L_c$  on measurement results. Only  $V_{off}$  needs to be predetermined for accurate measurement, which will be presented in the next subsection.

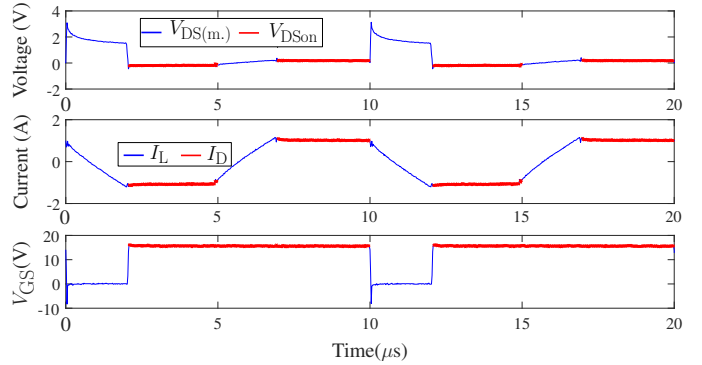
### C. $V_{off}$ calibration

In order to calibrate oscilloscope offset voltage  $V_{off}$ ,  $L$  and  $C_L$  are disconnected from the measurement circuit in Fig. 2b. When DUT (SiC-MOSFET) switches at 100kHz and  $V_{DC} = 200V$ , obtained device  $V_{DS(m.)}$ ,  $I_D$  and  $V_{GS}$  is shown in Fig. 10.

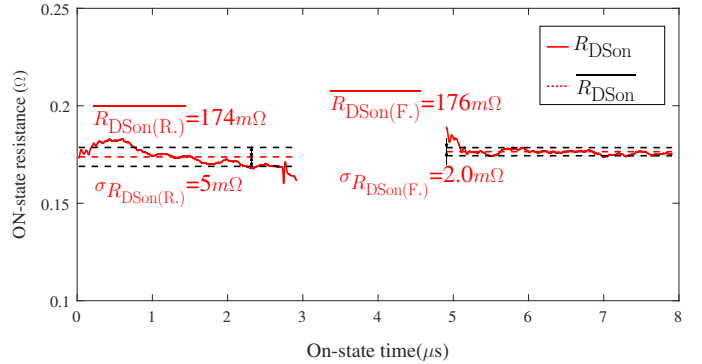
When  $V_{GS}$  equals to 16V, DUT is in ON-state. As there is no current flowing through DUT, both of measured  $I_D$  and  $V_{DSon}$  should be zero. The above measurement process is

TABLE IV:  $V_{off}$  calibrated results on both voltage and current measurement

|              | $\mu$ (mV) | $\sigma$ (mV) | $V_{FS}$ (V)  | $\frac{\mu}{V_{FS}}$ |
|--------------|------------|---------------|---------------|----------------------|
| $V_{off}(V)$ | -59        | 3             | 5 (0.5V/div.) | 1.2%                 |
| $V_{off}(I)$ | 27         | 0.6           | 5 (0.5V/div.) | 0.5%                 |



(a) Measured waveforms



(b)  $R_{DSon(R.)}$  and  $R_{DSon(F.)}$  of one switching period

Fig. 11: SiC-MOSFET reverse and forward ON-state resistance measurement results when device switches at 100kHz by proposed TZCM

repeated 20 times by connecting and disconnecting voltage and current probes. Therefore,  $V_{off}$  mean value ( $\mu$ ) and standard derivation ( $\sigma$ ) on both voltage ( $V_{off}(V)$ ) and current ( $V_{off}(I)$ ) measurement are obtained and they are compared with each oscilloscope channel full range value ( $V_{FS}$ ) in TABLE IV.

It can be concluded that obtained  $V_{off}$  is consistent by a small  $\sigma$  value. Meanwhile, obtained  $\frac{\mu}{V_{FS}}$  shows relative voltage offset error to channel full range voltage, which might be different in different manufacturers. After compensation,  $\sigma$  remains an unpredictable error source. However, its influence on measurement results is less than 1% ( $g_{V_{off}} \times \sigma = 0.75\%$ ).

After calibrating  $V_{off}$ ,  $R_{DSon}$  of both SiC-MOSFET and GaN-HEMT are obtained when they operate continuously in power converter.

## IV. MEASUREMENT RESULTS

### A. SiC-MOSFET

In order to validate the proposed TZCM method,  $R_{DSon}$  of the same SiC-MOSFET is measured when device is switching



at 100kHz ( $D_{DUT} = 80\%$ ),  $V_{DC} = 200V$  to compare with its values obtained in Fig. 7c. Obtained device  $V_{DS(m)}$ ,  $I_L$  and  $V_{GS}$  waveform are shown in Fig. 11a under sub-mode 3 of TZCM. When  $V_{GS} = 16V$ ,  $V_{DSon}$  and  $I_D$  can be obtained from measured  $V_{DS(m)}$  and  $I_L$  waveforms. Therefore, both  $R_{DSon(R)}$  and  $R_{DSon(F)}$  can be measured simultaneously at one switching period under constant current.

As compared in Fig. 11b, obtained  $\overline{R_{DSon(R)}}$  is about  $174m\Omega$ , and its  $\sigma_{R_{DSon(R)}}$  is about  $5m\Omega$ , which is 2.9% to  $\overline{R_{DSon(R)}}$  value. Obtained  $\overline{R_{DSon(F)}}$  is about  $176m\Omega$ , and its  $\sigma_{R_{DSon(F)}}$  is about  $2.0m\Omega$ , which is 1.1% to  $\overline{R_{DSon(F)}}$  value. Both  $\overline{R_{DSon(R)}}$  and  $\overline{R_{DSon(F)}}$  are slightly increased (7.4% and 1.7%) in comparison with their values shown in TABLE. III, which may be due to DUT junction temperature  $T_j$  difference when it is operated at 100kHz. Measurement consistency and accuracy of the proposed measurement circuit and TZCM method can be verified by those results.

## B. GaN-HEMT

1) *Single-pulse mode*: In order to investigate GaN transistor  $R_{DSon(R)}$  and  $R_{DSon(F)}$  with  $t_{on}$ , its dynamic  $R_{DSon}$  under both reverse and forward conduction is measured at first under single-pulse mode by the same method presented in section II-B.

A GaN-HEMT (GS66502B, 650V/7.5A,  $V_{th} = 1.3V$ ) with similar static  $R_{DSon}$  of around  $200m\Omega$  is characterised when  $t_{off}$  of Fig. 5 is set to be  $10ms$  and  $10s$ . As shown in Fig. 12a, in comparison with device static  $R_{DSon}$  value ( $0.195\Omega$ ), device dynamic  $R_{DSon}$  value can increase to 50% bigger and it increases more with longer  $t_{off}$ . It is also observed in the measurement results that obtained  $R_{DSon(F)}$  corresponds well to the  $R_{DSon(R)}$  value on the common  $t_{on}$  range ( $800ns$  to  $3\mu s$ ), which confirms that dynamic  $R_{DSon}$  value decreases to static  $R_{DSon}$  value with  $t_{on}$ . This result conforms to reported GaN device dynamic  $R_{DSon}$  variation in the literature [17] and can be used as a reference to verify measurement results when device is operated in high frequency switching converter. It is also shown in the results that GaN-HEMT does not have body-diode to lower its  $R_{DSon(R)}$  than  $R_{DSon(F)}$ . Obtained device dynamic  $R_{DSon}$  under both reverse and forward conduction is due to trapped charge.

Another GaN gate injection transistor (GIT, PGA26E19BA, 600V/13A) has been tested with the same method under conditions:  $V_{DS} = 200V$ ,  $I_D = 2A$  and  $t_{off} = 10s$ . As presented in Fig. 12b, it reveals again that obtained  $R_{DSon(R)}$  corresponds to  $R_{DSon(F)}$  value on the common  $t_{on}$  range, owing to the accuracy of proposed measurement circuit. For this GIT, dynamic  $R_{DSon}$  increases twice bigger than its static  $R_{DSon}$  value when  $t_{on}$  is less than  $100ns$ , revealing a non-negligible effect on device conduction losses.

2) *Continuous mode*: When device is switching at 1MHz ( $D_{DUT} = 50\%$ ) and  $V_{DC} = 200V$ , dynamic  $R_{DSon}$  of the same GaN-HEMT is then measured by the proposed TZCM and conventional TCM method, where the measurement results are shown in Fig. 13. It can be noted that when DUT is fully turned ON at  $V_{GS} = 6V$ , obtained  $V_{DSon}$  is negative in all the experimental results, which confirms that DUT is under

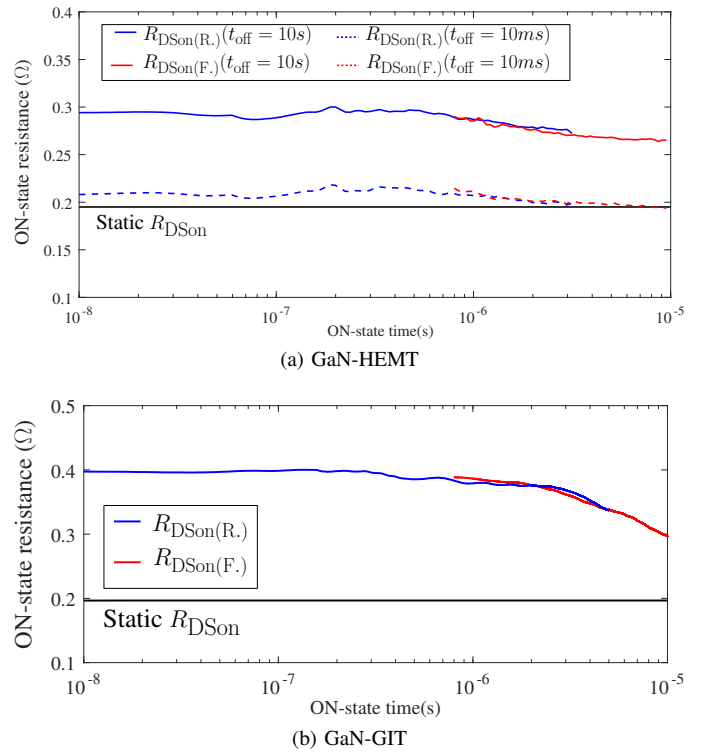


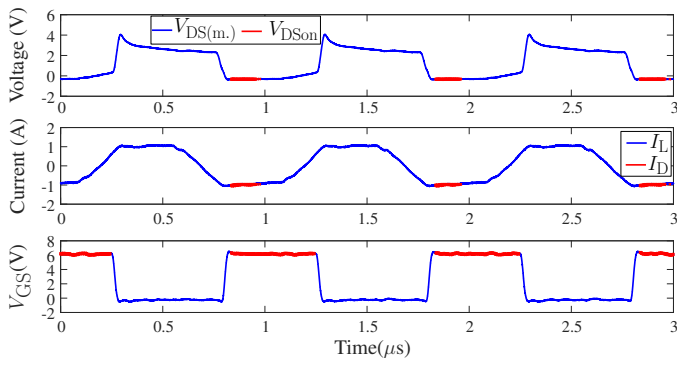
Fig. 12: Reverse and forward dynamic  $R_{DSon}$  of different GaN transistors

reverse conduction and it realizes ZVS soft switching at turn-ON transition, as its  $C_{oss}$  is fully discharged by  $I_L$  during deadtime.

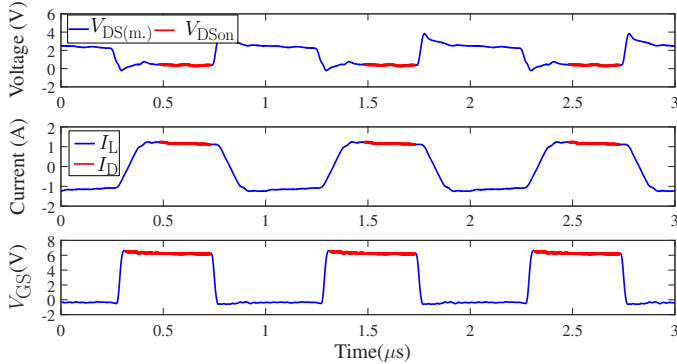
By using TZCM method,  $R_{DSon(R)}$  is obtained under constant reverse  $I_D$  at sub-mode 1 (see Fig. 13a) and  $R_{DSon(F)}$  is obtained under constant forward  $I_D$  at sub-mode 2 (see Fig. 13b). By using conventional TCM method, device  $R_{DSon}$  is obtained when  $I_D$  is around 1A in both reverse and forward conduction (see Fig. 13c). Obtained  $R_{DSon}$  and their mean value  $\overline{R_{DSon}}$  over the chosen conduction time by the two methods are then compared in Fig. 14.  $\sigma_{R_{DSon}}$  is inferior to  $3m\Omega$  in all the obtained data, which confirms again the measurement consistency by using the proposed circuit. Therefore,  $\overline{R_{DSon}}$  can be used to compare the measurement accuracy of different methods.

By conventional TCM method, obtained GaN-HEMT dynamic  $\overline{R_{DSon(R)}}$  is  $308m\Omega$  and  $\overline{R_{DSon(F)}}$  is  $365m\Omega$ . The difference ( $\Delta R = \overline{R_{DSon(R)}} - \overline{R_{DSon(F)}}$ ) is  $-56m\Omega$ , which is about -18.5% to  $\overline{R_{DSon(R)}}$  value. The increase of device dynamic ON-state resistance value during one switching period with ON-state time does not agree with GaN device physics shown in Fig. 12a. As shown in section III-A, influence of  $t_{dk}$  and  $L_c$  on measurement sensitivity becomes critical under fast  $I_L$  transition (more than  $5A/\mu s$  as shown in Fig. 13c). This negative ON-state resistance difference can be further explained by eq.(2), where the term  $\frac{dI_D}{dt}$  lowers apparent  $V_{DSon(m)}$  value when DUT is in reverse conduction and increases  $V_{DSon(m)}$  value when DUT is in forward conduction.

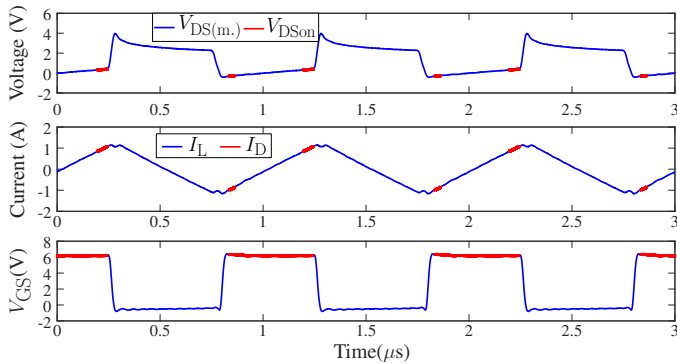
In comparison, by proposed TZCM, obtained GaN-HEMT  $\overline{R_{DSon(R)}}$  is  $331m\Omega$  and  $\overline{R_{DSon(F)}}$  is  $327m\Omega$  at one period.



(a) Device switches at sub-mode 1 of TZCM



(b) Device switches at sub-mode 2 of TZCM



(c) Device switches at TCM

Fig. 13: GaN-HEMT dynamic ON-state resistance measurement results by proposed TZCM and by conventional TCM when device switches at 1MHz

$\Delta R$  is only  $4m\Omega$ , which is about 1.2% to  $\overline{R_{DSon(R.)}}$  value. This slight decrease of device dynamic  $R_{DSon}$  with ON-state time at one switching period conforms to obtained GaN device dynamic ON-state resistance values in Fig. 12a, which also demonstrates the advantage of proposed TZCM method over conventional TCM method on measurement accuracy when circuit  $L_c$  cannot be ignored in high frequency power converter. It is to be noted that  $L_c$  can be reduced by using an all-integration PCB board. Nevertheless, as presented in eq.(5), designers would still have unavoidable  $g_{L_c}$  measurement issue depending on device switching frequency and  $R_{DSon}$  value by using conventional TCM method.

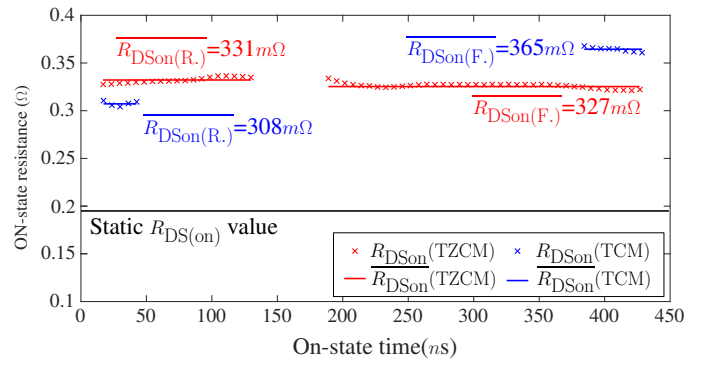


Fig. 14: GaN-HEMT dynamic ON-state resistance comparison between TZCM and TCM

## V. CONCLUSION

In this paper, a measurement circuit is proposed to measure GaN transistor dynamic ON-state resistance  $R_{DSon}$  when device is operated in high frequency converters. The measurement circuit is constituted by a standard H-bridge to control device switching (DSC) and a voltage clamping circuit (VCC) to reduce measured voltage from full DC bus voltage to a few volts, so as to improve measurement resolution. In comparison with different state-of-the-art of VCC, the proposed one has a simple structure (only three components), good dynamic response (10 ns) and can be used to measure power transistor both reverse and forward  $R_{DSon}$  with robust accuracy, which is suitable for device application in soft switching circuit. The measurement circuit is then validated by measuring on SiC-MOSFET with constant  $R_{DSon}$  value when device is under both reverse and forward conduction.

Afterwards, influence of unavoidable common parasitic inductance  $L_c$  between DSC and VCC, voltage and current probes deskew ( $t_{dk}$ ) and oscilloscope offset voltage ( $V_{off}$ ) on measurement sensitivity is analyzed, which shows potential sensitivity issue in conventional device  $R_{DSon}$  measurement by triangle current mode (TCM) method when device operates in high frequency converter. In order to eliminate the influence of  $L_c$  and  $t_{dk}$  on measurement sensitivity, a trapezoidal current mode (TZCM) method is proposed. By adding a phase shift between two phases of a H-bridge, transistor  $R_{DSon}$  can be obtained under an almost constant drain current. Therefore, only  $V_{off}$  needs to be calibrated in TZCM method, in which its value can be easily obtained by a measurement when DUT operates without current.

Reverse and forward ON-state resistances ( $R_{DSon(R.)}$  and  $R_{DSon(F.)}$ ) of the same SiC-MOSFET are measured by TZCM when device operates at 100kHz. Measurement results conform to their values obtained by a curve tracer, which validates consistency and accuracy of proposed TZCM method. Following that, when device switches at 1MHz, GaN device dynamic  $R_{DSon}$  is measured by both TZCM method and conventional TCM method. It is shown in the measurement results the sensitivity issue caused by  $t_{dk}$  and  $L_c$  in conventional TCM method under fast transition of drain current, which causes a non-physical device dynamic  $R_{DSon}$  increase with ON-state time. The advantage of proposed TZCM method on

measurement accuracy is thus justified.

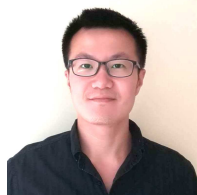
Based on the results of the paper, a GaN device model taking into consideration of device dynamic  $R_{\text{DSon}}$  evaluation under different operation conditions can be built and validated, which will be the subject of future communications.

#### ACKNOWLEDGMENT

This work was funded by the UK Engineering and Physical Sciences Research Council (EPSRC) through research grant [EP/K035304/1 and EP/R004390/1]. The authors would also like to thank the support from University of Lille for the collaborated research work through State Region Plan Contract Intelligent Integrated Energy Converter (CPEP-CE2I) project.

#### REFERENCES

- [1] W. Zhang, F. Wang, D. J. Costinett, L. M. Tolbert, and B. J. Blalock, "Investigation of Gallium Nitride Devices in High-Frequency LLC Resonant Converters," *IEEE Transactions on Power Electronics*, vol. 32, pp. 571–583, Jan 2017.
- [2] M. Guz, D. Sanderlin, B. H. Sin, M. de Rooij, T. McDonald, P. Le, A. Young, M. Seeman, and J. Walker, "IEEE ITRW Working Group Position Paper-System Integration and Application: Gallium Nitride: Identifying and Addressing Challenges to Realize the Full Potential of GaN in Power Conversion Applications," *IEEE Power Electronics Magazine*, vol. 5, pp. 34–39, June 2018.
- [3] S. Jiang, K. B. Lee, I. Guiney, P. F. Miaja, Z. H. Zaidi, H. Qian, D. J. Wallis, A. J. Forsyth, C. J. Humphreys, and P. A. Houston, "All-GaN-Integrated Cascode Heterojunction Field Effect Transistors," *IEEE Transactions on Power Electronics*, vol. 32, pp. 8743–8750, Nov 2017.
- [4] M. Fu, C. Fei, Y. Yang, Q. Li, and F. Lee, "Optimal Design of Planar Magnetic Components for A Two-Stage GaN-Based DC/DC Converter," *IEEE Transactions on Power Electronics*, pp. 1–1, 2018.
- [5] M. S. Haque and S. Choi, "Prognosis of enhance mode gallium nitride high electron mobility transistors using on-state resistance as fault precursor," in *2017 IEEE Energy Conversion Congress and Exposition (ECCE)*, pp. 1988–1994, Oct 2017.
- [6] M. A. Eleffendi and C. M. Johnson, "In-Service Diagnostics for Wire-Bond Lift-off and Solder Fatigue of Power Semiconductor Packages," *IEEE Transactions on Power Electronics*, vol. 32, pp. 7187–7198, Sep. 2017.
- [7] W. Saito, Y. Kakiuchi, T. Nitta, and Y. Saito et al., "Field-Plate Structure Dependence of Current Collapse Phenomena in High-Voltage GaN-HEMTs," *Electron Device Letters, IEEE*, vol. 31, no. 7, pp. 659–661, 2010.
- [8] M. Uren and M. Kuball, "GaN transistor reliability and instabilities," in *Advanced Semiconductor Devices Microsystems (ASDAM), 2014 10th International Conference on*, pp. 1–8, Oct 2014.
- [9] H. Chandrasekar, M. J. Uren, A. Eblabla, H. Hirshy, M. A. Casbon, P. J. Tasker, K. Elgaid, and M. Kuball, "Buffer-Induced Current Collapse in GaN HEMTs on Highly Resistive Si Substrates," *IEEE Electron Device Letters*, vol. 39, pp. 1556–1559, Oct 2018.
- [10] B. J. Galapon, A. J. Hanson, and D. J. Perreault, "Measuring Dynamic On Resistance in GaN Transistors at MHz Frequencies," in *2018 IEEE 19th Workshop on Control and Modeling for Power Electronics (COMPEL)*, pp. 1–8, June 2018.
- [11] N. Badawi, O. Hilt, E. Bahat-Treidel, J. Böcker, J. Würfl, and S. Dieckhoff, "Investigation of the Dynamic On-State Resistance of 600 V Normally-Off and Normally-On GaN HEMTs," *IEEE Transactions on Industry Applications*, vol. 52, pp. 4955–4964, Nov 2016.
- [12] Y. Cai, A. J. Forsyth, and R. Todd, "Impact of GaN HEMT dynamic on-state resistance on converter performance," in *2017 IEEE Applied Power Electronics Conference and Exposition (APEC)*, pp. 1689–1694, March 2017.
- [13] F. Yang, C. Xu, and B. Akin, "Quantitative Analysis of Different Operating Conditions' Effect on Dynamic On-Resistance in Enhancement-Mode GaN HEMTs," in *2018 IEEE 6th Workshop on Wide Bandgap Power Devices and Applications (WiPDA)*, pp. 134–140, Oct 2018.
- [14] T. Foulkes, T. Modeer, and R. C. N. Pilawa-Podgurski, "Developing a standardized method for measuring and quantifying dynamic on-state resistance via a survey of low voltage GaN HEMTs," in *2018 IEEE Applied Power Electronics Conference and Exposition (APEC)*, pp. 2717–2724, March 2018.
- [15] K. Li, P. L. Evans, and C. M. Johnson, "Characterisation and Modeling of Gallium Nitride Power Semiconductor Devices Dynamic On-State Resistance," *IEEE Transactions on Power Electronics*, vol. 33, pp. 5262–5273, June 2018.
- [16] B. Lu, T. Palacios, D. Risbud, S. Bahl, and D. Anderson, "Extraction of Dynamic On-Resistance in GaN Transistors: Under Soft- and Hard-Switching Conditions," in *Compound Semiconductor Integrated Circuit Symposium (CSICS), 2011 IEEE*, pp. 1–4, Oct 2011.
- [17] R. Li, X. Wu, S. Yang, and K. Sheng, "Dynamic on-State Resistance Test and Evaluation of GaN Power Devices Under Hard- and Soft-Switching Conditions by Double and Multiple Pulses," *IEEE Transactions on Power Electronics*, vol. 34, pp. 1044–1053, Feb 2019.
- [18] D. Han and B. Sarlioglu, "Deadtime Effect on GaN-Based Synchronous Boost Converter and Analytical Model for Optimal Deadtime Selection," *Power Electronics, IEEE Transactions on*, vol. 31, pp. 601–612, Jan 2016.
- [19] R. Gelagaev, P. Jacqmaer, and J. Driesen, "A Fast Voltage Clamp Circuit for the Accurate Measurement of the Dynamic ON-Resistance of Power Transistors," *Industrial Electronics, IEEE Transactions on*, vol. 62, pp. 1241–1250, Feb 2015.
- [20] K. Li, P. Evans, and M. Johnson, "SiC/GaN power semiconductor devices: a theoretical comparison and experimental evaluation under different switching conditions," *IET Electrical Systems in Transportation*, vol. 8, no. 1, pp. 3–11, 2018.
- [21] M. Guacci, D. Bortis, and J. W. Kolar, "On-state voltage measurement of fast switching power semiconductors," *CPSS Transactions on Power Electronics and Applications*, vol. 3, pp. 163–176, June 2018.
- [22] Tektronix, "Understanding Key High-Performance Oscilloscope Specifications," 2002.
- [23] Z. Zhang, B. Guo, F. F. Wang, E. A. Jones, L. M. Tolbert, and B. J. Blalock, "Methodology for Wide Band-Gap Device Dynamic Characterization," *IEEE Transactions on Power Electronics*, vol. 32, pp. 9307–9318, Dec 2017.



**Ke Li (M'14)** received BEng and MEng degrees in electrical engineering from Southwest Jiaotong University, China, in 2008 and 2011 respectively, and the Eng.degree from Ecole Centrale de Marseille, France, in 2011. He received the Ph.D degree in electrical engineering from University of Lille, France, in 2014.

From 2015 to 2019, he was Research Fellow at the University of Nottingham, UK. In 2019, he was appointed as Assistant Professor in power electronics, machines and drives, Coventry University, UK.

His research interests include wide-bandgap (SiC/GaN) power semiconductor devices integration to high power-density power converters, power converters electrothermal and electromagnetic modelling and power converters electromagnetic interference mitigation.



**Arnaud Videt (M'09)** received the Ph.D degree in electrical engineering from Ecole Centrale de Lille, France, in 2008, and joined Schneider Toshiba Inverter, Pacy-sur-Eure, France, where his research focused on motor drive converter topologies and modulation strategies. Since 2010, he is Associate Professor with the L2EP laboratory, University of Lille, France. His current research interests include wide-bandgap power devices and electromagnetic compatibility issues in power converters.



**Nadir Idir (M'93)** received the Ph.D. degree electrical engineering from the University of Lille 1, France, in 1993.

He is a Full Professor with IUT A of the University of Lille 1, where he teaches power electronics and Electromagnetic Compatibility (EMC). Since 1993, he has been with the Laboratory of Electrical Engineering and Power Electronics (L2EP) of the University of Lille 1. His research interests include, design methodologies for HF switching converters, power devices (SiC and GaN), electromagnetic inter-

ference (EMI) in static converters, HF modelling of the passive components, EMI filter design methodologies for power converters.



**Paul Evans** received the MEng degree in Electrical and Electronic Engineering, and the PhD degree in Electrical engineering from the University of Nottingham, UK, in 2007, and 2011 respectively. In 2010 he became a Research Fellow, was appointed Assistant Professor in 2013 and then Associate Professor in 2019 at the same institution. His expertise lies in the application of accelerated computational modelling techniques to the simulation of power electronic systems and his work on extraction of compact thermal models was awarded the IEEE

Transactions on Power Electronics second prize paper in 2013. He currently leads the Virtual Prototyping work in the EPSRC Centre for Power Electronics.



**Christopher Mark Johnson (M'90)** received the BA degree in engineering and the PhD degree in electrical engineering from the University of Cambridge, UK, in 1986 and 1991 respectively.

From 1990 to 1992 he was a Research Associate at the University of Cambridge and in 1992 he was appointed Lecturer at the Newcastle University, UK, where his research included the design, analysis and characterisation of power semiconductor devices, resonant power conversion and instrumentation.

From 1998 to 2001 he managed the UK national programme on Silicon Carbide electronics and in 2000 he became Reader of Power Electronics at Newcastle University. In 2003, Professor Johnson was appointed as Rolls-Royce/RAEng Research Professor of Power Electronic Systems at the University of Sheffield and in 2006 he was appointed to a personal chair at the University of Nottingham, where he leads research into power semiconductor devices, power device packaging, reliability, thermal management, power module technologies and power electronic applications. He is Director of the UK Engineering and Physical Sciences Research Council (EPSRC) Centre for Power Electronics, which combines the UK's best academic talent to address the key research challenges underpinning power electronics and is leader of the Advanced Propulsion Centre (APC) Thematic Spoke in Power Electronics.